Journal of Catalysis **198,** 256–265 (2001)
doi:10.1006/jcat.2000.3137, available online at http://www.idealibrary.com on IDEAL®

Influence of the Nature of Residual Alkali Cations on the Catalytic Activity of Zeolites X, Y, and EMT in their Brønsted Acid Forms

Michaela Weihe,* Michael Hunger,* Marcus Breuninger,* Hellmut G. Karge,† and Jens Weitkamp*,[1]

*Institute of Chemical Technology, University of Stuttgart, D-70550 Stuttgart, Germany; and †Fritz Haber Institute of the Max Planck Society, Faradayweg 4-6, D-14195 Berlin, Germany

Received July 31, 2000; revised November 29, 2000; accepted November 29, 2000; published online February 15, 2001

Lanthanum-exchanged zeolites X, Y, and EMT, containing either sodium or potassium as residual cations, were used as catalysts in two acid-catalyzed hydrocarbon reactions, viz. the disproportionation of ethylbenzene and the isomerization of *n*-octane (for the latter reaction, Pd/γ-Al_2O_3 was admixed to the acid zeolites to make the catalysts bifunctional). All pairs of La*M*-type zeolites (where *M* stands for Na or K) showed remarkable activity differences, the LaK form being always less active than the LaNa form. IR and ^{1}H NMR spectroscopy revealed that, for a given zeolite type and degree of lanthanum exchange, the concentration of bridging hydroxyl groups in the large cages was at least 20% lower than that for the LaK form. ^{139}La NMR spectroscopy indicated that the concentration of lanthanum ions in the large cages of the as-exchanged LaK forms was always lower than that in the corresponding LaNa forms. Surprisingly, already in the as-exchanged LaK forms, some La^{3+} migration into the small cages appears to occur, and this was corroborated by framework strains indicated by ^{29}Si and ^{27}Al NMR. It is proposed that potassium cations in the large cages cause an enhanced migration of lanthanum cations into the small cages and a preferential formation of Brønsted acid sites in these small cages during the thermal dehydration of lanthanum cations (Hirschler–Plank mechanism). A similar effect was found in HNaY and HKY zeolites: The presence of the bulkier potassium cations causes a significant diminution of the accessible Brønsted acid sites in the large cages and of the catalytic activity. Overall, one must conclude from these results that in zeolites possessing both large and small cages, the nature of the residual alkali cations can exert a pronounced influence on the local distribution of the Brønsted acid sites, regardless of how these sites were generated.

Key Words: **faujasite; zeolite EMT; ethylbenzene disproportionation; *n*-octane isomerization; solid-state NMR spectroscopy; Brønsted acid sites; lanthanum migration.**

INTRODUCTION

A broad variety of hydrocarbon reactions are known to be catalyzed by zeolites containing Brønsted acid sites. Industrially relevant examples are catalytic cracking of vacuum distillates from petroleum, the alkylation of aromatics with alkenes, and the isomerization and transalkylation of alkylaromatics. For instance, the transalkylation (or disproportionation) of ethylbenzene has been shown by Karge *et al.* (1) to be a valuable test reaction for acidic zeolite catalysts. In another class of industrially important catalysts, a solid in its Brønsted acid form is modified by a metal possessing hydrogenation/dehydrogenation activity. In such bifunctional catalysts, one of the main roles of the metal is to effect a rapid interconversion of alkanes and alkenes, while the steps at the Brønsted acid sites are often rate and selectivity controlling. Typical hydrocarbon reactions occurring on bifunctional zeolites are the skeletal isomerization and hydrocracking of alkanes (2) or naphthenes (3).

There are several well-established methods for generating Brønsted acid sites in the pores or cavities of a zeolite. Among these are the introduction of ammonium ions followed by thermal deammoniation and the introduction of multivalent metal cations, such as Mg^{2+}, Ca^{2+}, La^{3+}, or a mixture of rare-earth cations (RE^{3+}), by ion exchange in aqueous suspension followed by thermal dehydration. RE^{3+}-containing faujasites are playing an important role in fluid catalytic cracking (FCC) of heavy petroleum distillates (4, 5). According to the generally accepted Hirschler–Plank mechanism (6), Brønsted acid sites are formed in zeolites containing multivalent cations upon thermal removal of most of the water initially present in the pores: In the local electrostatic fields, a water molecule dissociates, and the proton formed together with a negatively charged oxygen framework gives a so-called bridging hydroxyl group that is the catalytically active Brønsted site.

O'Donoghue and Barthomeuf (7) and Chen *et al.* (8) studied H*M*-faujasites (where *M* stands for various alkali cations) prepared by thermal deammoniation of the respective NH_4M-faujasites. According to Sanderson's principle of electronegativity equalization, the strength of Brønsted acid sites depends on the nature of the alkali cation *M* and is expected to decrease in the series HLiY > HNaY > HKY > HRbY (7, 8). Indeed, O'Donoghue and Barthomeuf (7) found a decrease of the catalytic activity in the dehydration of 2-propanol (to diisopropyl ether and propene) at 388 K in the same order. Chen *et al.* (8) interpreted differences

[1] To whom correspondence should be addressed. Fax: +49/711/685-4065. E-mail: jens.weitkamp@po.uni-stuttgart.de.

0021-9517/01 $35.00

in the amount of strongly adsorbed pyridine molecules in zeolites HNaY and HKY in terms of different strengths of the Brønsted and Lewis acid sites in these zeolites, i.e., in terms of decreasing partial charges residing at the hydrogen and the aluminum atoms, respectively. Both groups of authors tacitly assumed that in their HNaY and HKY zeolites, equal amounts of acid sites that are accessible for the reactant 2-propanol and the probe pyridine are available. As will be shown in the present article, doubts are justified as to whether such an assumption is valid. In zeolites possessing both small and spacious cages, such as faujasite or zeolite EMT, the locus of catalytic conversion of organic substrates is almost always restricted to the large cages. Obviously, the distribution of acid sites between the small and large cages is an important parameter for the in-depth characterization of such catalysts. Here we report on large differences observed in the catalytic activities of seemingly identical La*M* and H*M* zeolites (where *M* stands again for alkali cations) in two different hydrocarbon reactions, viz. the disproportionation of ethylbenzene and the isomerization of *n*-octane. Infrared (9) and multinuclear solid-state NMR spectroscopy (10–12) were used to characterize the La*M*X, La*M*Y, La*M*EMT, and H*M*Y materials.

EXPERIMENTAL SECTION

Materials

Zeolites NaX (sample X/1; $n_{Si}/n_{Al} = 1.3$) and NaY (sample Y/2; $n_{Si}/n_{Al} = 2.6$) were kindly supplied by Union Carbide Corporation, Tarrytown, NY. Zeolites Y (sample Y/3; $n_{Si}/n_{Al} = 4.5$) and EMT (sample EMT/4; $n_{Si}/n_{Al} = 4.3$) were synthesized according to published recipes (13) using, respectively, 15-crown-5 ether (14) and 18-crown-6 ether (14–16) as structure-directing agents. To remove the templates from the latter materials, they were calcined in a dried flow of nitrogen-diluted air (95 vol.% N_2 and 5 vol.% O_2) for 25 h at 813 K.

For the preparation of all La*M* zeolites, the pure sodium forms were first prepared by ion exchange in a surplus of 0.1 N $NaNO_3$ solution in water at 298 K. These materials were then further ion-exchanged four times with a 0.1 N aqueous $La(NO_3)_3$ solution at 353 K, yielding the respective LaNa zeolites. The products were thoroughly washed with demineralized water and dried at 298 K. For the preparation of the LaK zeolites, aliquots of the pure sodium forms were ion-exchanged eight times with a 0.1 N solution of KNO_3 in water, washed with demineralized water, and dried at 298 K. The resulting potassium forms were then subjected to the same ion exchange procedure with $La(NO_3)_3$ as the sodium forms (vide supra). One gram of as-exchanged LaNa and LaK zeolite X/1 were backexchanged with a large surplus of 0.1 N aqueous $NaNO_3$ solution. To prepare the H*M*Y/2 samples, zeolite NaY ($n_{Si}/n_{Al} = 2.6$, Union Carbide Corporation, Tarrytown), was ion-exchanged in a 1 M aqueous solution of NH_4NO_3 to a final n_{Na}/n_{Al} ratio of <0.001. The resulting NH_4Y zeolite was backexchanged with $NaNO_3$ or KNO_3, leading to ion exchange degrees of $n_{Na}/n_{Al} = 0.28$ (72HNaY/2), $n_{Na}/n_{Al} = 0.45$ (55HNaY/2), $n_K/n_{Al} = 0.25$ (75HKY/2), and $n_K/n_{Al} = 0.46$ (54HKY/2).

TABLE 1

Chemical Compositions of the La*M* and H*M* Zeolites (Determined by ICP-AES) and Framework n_{Si}/n_{Al} Ratios of the As-Exchanged Samples (Determined by ^{29}Si MAS NMR Spectroscopy)

Sample designation	Chemical composition	Framework n_{Si}/n_{Al}
LaNaX/1	$La_{25.0}\ Na_{6.0}\ Si_{109.4}\ Al_{82.6}\ O_{384.0}$	1.3
LaKX/1	$La_{23.1}\ K_{7.1}\ Na_{0.4}\ Si_{111.5}\ Al_{80.5}\ O_{384.0}$	1.3
LaNaY/2	$La_{12.7}\ Na_{15.0}\ Si_{138.8}\ Al_{53.2}\ O_{384.0}$	2.6
LaKY/2	$La_{12.2}\ K_{15.0}\ Na_{0.8}\ Si_{139.5}\ Al_{52.5}\ O_{384.0}$	2.6
LaNaY/3	$La_{8.0}\ Na_{10.5}\ Si_{157.5}\ Al_{34.5}\ O_{384.0}$	4.5
LaKY/3	$La_{7.4}\ K_{11.2}\ Na_{2.0}\ Si_{156.6}\ Al_{35.4}\ O_{384.0}$	4.5
LaNaEMT/4	$La_{4.4}\ Na_{4.8}\ Si_{78.2}\ Al_{17.8}\ O_{192.0}$	4.3
LaKEMT/4	$La_{4.7}\ K_{3.5}\ Na_{0.4}\ Si_{78.0}\ Al_{18.0}\ O_{192.0}$	4.3
72HNaY/2	$H_{38.3}\ Na_{14.9}\ Si_{138.8}\ Al_{53.2}\ O_{384.0}$	2.6
75HKY/2	$H_{39.9}\ K_{13.3}\ Si_{138.8}\ Al_{53.2}\ O_{384.0}$	2.6
55HNaY/2	$H_{29.3}\ Na_{23.9}\ Si_{138.8}\ Al_{53.2}\ O_{384.0}$	2.6
54HKY/2	$H_{28.7}\ K_{24.5}\ Si_{138.8}\ Al_{53.2}\ O_{384.0}$	2.6

All La*M* and H*M* zeolites were analyzed by atomic emission spectroscopy with an inductively coupled plasma (ICP-AES, Perkin–Elmer, Plasma 400). The results of the chemical analyses are listed in Table 1. ^{29}Si MAS NMR spectroscopy was applied to determine the framework n_{Si}/n_{Al} ratios of the materials (17). These values are given in Table 1 as well.

Catalysis

The catalytic experiments were carried out at atmospheric pressure in a flow-type apparatus equipped with a fixed-bed reactor. Nitrogen and hydrogen were used, respectively, as carrier gases in the ethylbenzene disproportionation and isomerization of *n*-octane. Periodically, samples of the product stream were analyzed by capillary gas chromatography. Ethylbenzene (E-Bz) and *n*-octane (*n*-Oc), both analytical grade, were purchased from Merck, Darmstadt. Whereas *n*-octane was used without further purification, ethylbenzene was passed over a column filled with Al_2O_3 to remove polar impurities. The catalysts were pressed binder-free, crushed, and sieved into particles with a diameter between 0.2 and 0.3 mm. Prior to the ethylbenzene disproportionation and the *n*-octane conversion, the catalysts were heated *in situ* with a rate of 3 K/min to the final temperature of 523 and 673 K (La*M* and H*M* zeolites, respectively) and purged at this temperature with dry nitrogen and hydrogen (flow rate = 2.4 l/h), respectively, for 12 h. The ethylbenzene disproportionation was carried out at a temperature of 453 K, with 290 mg of catalyst and

a modified residence time of $W/F_{E\text{-}Bz} = 290$ g · h/mol. For the *n*-octane conversion, 290 mg of zeolite were carefully mixed with 870 mg of 0.1 wt.% palladium on γ-alumina (0.1 Pd/γ-Al_2O_3). The resulting mixed solids are denoted as Pd/La*M*Y/2 and Pd/H*M*Y/2. *n*-Octane hydroconversion was performed at temperatures of 473 and 513 K with $W/F_{n\text{-}Oc} = 1000$ g · h/mol and a hydrogen flow of 2.4 l/h. The absence of hydrogenolysis on the noble metal was ascertained in a separate test in which the reactor contained 870 mg of 0.1 Pd/γ-Al_2O_3.

Spectroscopic Characterization

IR spectra were recorded using a Perkin–Elmer IR spectrometer 325 in the transition mode. For this purpose the samples were pressed into self-supporting wafers (6 to 10 mg · cm^{-2}). Details of the IR-spectroscopic methods are given elsewhere (9). Solid-state NMR experiments were carried out on a Bruker MSL 400 spectrometer at resonance frequencies of 400.13 MHz for ^{1}H, 104.3 MHz for ^{27}Al, 79.5 MHz for ^{29}Si, and 56.5 MHz for ^{139}La. For the ^{1}H and ^{27}Al MAS NMR studies a standard 4-mm double-bearing Bruker MAS probe with a rotation frequency of 10 kHz was used with single-pulse excitation corresponding to $\pi/2$ (^{1}H) and $\pi/6$ (^{27}Al) flip angles. A minimum of 200 scans for ^{1}H and 1000 scans for ^{27}Al NMR were accumulated for each MAS NMR spectrum with a recycle time of 10 s (^{1}H) and 500 ms (^{27}Al). ^{27}Al DOR NMR measurements were carried out with a standard Bruker DOR probe and a rotation frequency of the outer rotor of 1200 Hz. For ^{29}Si MAS NMR, a 7-mm double-bearing Bruker MAS standard probe was applied with a rotation frequency of 4 kHz, single-pulse excitation corresponding to $\pi/4$ and a recycle time of 10 s and 500 scans. The ^{139}La NMR spectra were recorded with a p_1–τ_1–p_2–τ_2 echo sequence with the phase cycle proposed by Kunwar *et al.* (18) using a static Bruker probe. A pulse length of $p_1 = p_2 = 0.8$ μs, a pulse delay of $\tau_1 = 10$ μs, and an acquisition delay of $\tau_2 = 8$ μs were chosen. For each ^{139}La NMR spectrum, 10,000 scans were recorded with a recycle delay of 200 ms. A hydrated zeolite LaNaY with a degree of lanthanum exchange of 20% was applied as external ^{139}La NMR intensity standard. The intensity standard used for ^{1}H MAS NMR was a calcined (673 K) zeolite NH_4NaY with a degree of ammonium exchange of 35%. Quantitative investigations were carried out with Fourier transformation in the absolute intensity mode. The chemical shifts are referenced to external standards, viz. tetramethyl silane for ^{1}H and ^{29}Si MAS NMR spectroscopy and 0.1 M aqueous $Al(NO_3)_3$ solution for ^{27}Al MAS NMR spectroscopy. IR and ^{1}H MAS NMR studies were performed on samples dehydrated for 12 h at 523 K (La*M* samples) or 673 K (H*M* samples) in vacuum ($p < 10^{-2}$ Pa). C_5NH_5 and C_5ND_5 (Aldrich Chemical Co.) were adsorbed at their respective vapor pressures at room temperature. Physisorbed pyridine was desorbed in vacuum ($p < 10^{-2}$ Pa) at room temperature (C_5ND_5,^{1}H NMR samples) and 425 K (C_5NH_5, IR samples).

RESULTS

Disproportionation of Ethylbenzene

The conversion of ethylbenzene on the four pairs of La*M* zeolites in dependence of time on stream is shown in Fig. 1. At these relatively low conversions, disproportionation

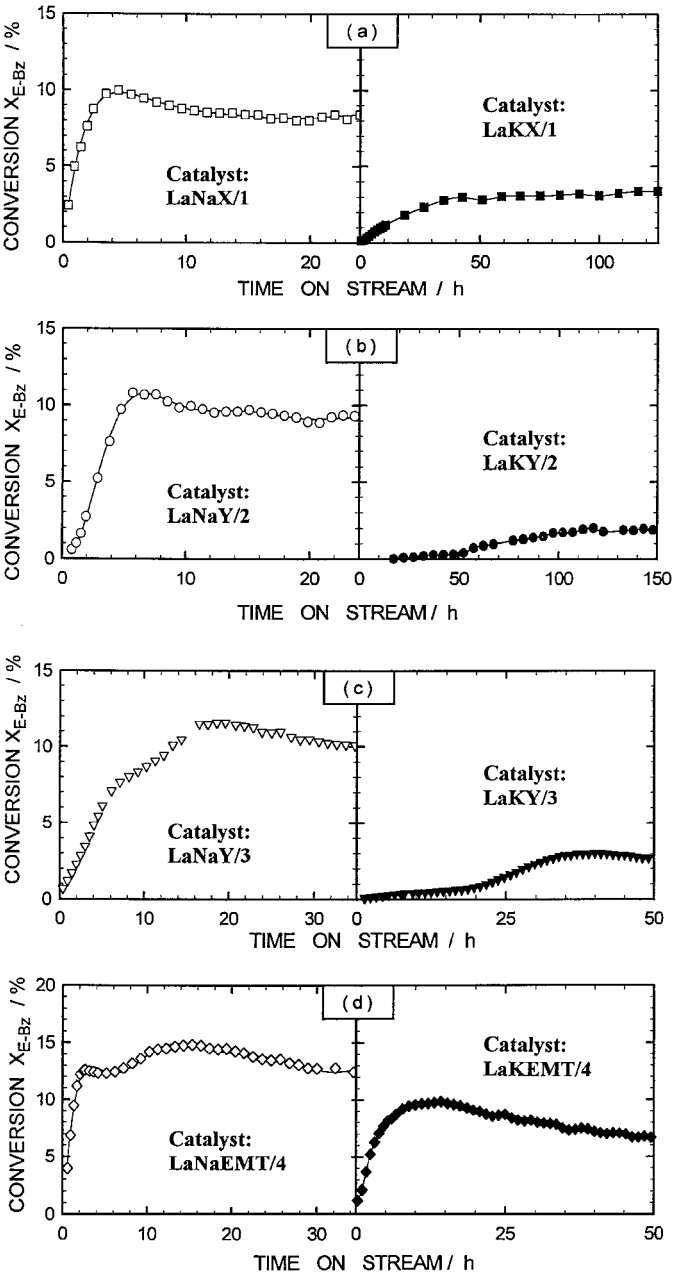

FIG. 1. Ethylbenzene disproportionation on zeolites La*M*X/1 (a), La*M*Y/2 (b), La*M*Y/3 (c), and La*M*EMT/4 (d). Conversion in dependence of time on stream at a reaction temperature of 453 K.

into benzene and the three diethylbenzene isomers was the sole reaction. As found earlier for other large-pore zeolites (19, 20), an induction period is observed in all cases; i.e., the ethylbenzene conversion initially increases up to certain value, whereupon a (quasi-)stationary state is reached in which the conversion remains constant (or decreases slowly, due to coke formation in the pores). The duration of the induction period varies drastically and assumes values from approximately 2 h (LaNaEMT/4) to more than 100 h (LaKY/2). Again in agreement with earlier reports (21), there is a qualitative correlation between the duration of the induction period and the height of the ethylbenzene conversion finally reached in the (quasi-stationary) state: The higher the latter, i.e., the more active the catalyst is, the shorter is the induction period.

The new and most relevant information comes from a comparison of the LaNa and LaK forms (left-hand and right-hand parts of Figs. 1a to 1d, respectively) of the zeolites: Not only are in all four cases the LaK forms less active in the (quasi-)stationary state, but the induction period on these catalysts is longer than on the respective LaNa forms. Listed in Table 2 (column 2) are the ethylbenzene conversions in the (quasi-)stationary state on La*M* zeolites. These figures represent the end-of-run values from Fig. 1, and as such they are somewhat ambiguous, especially in those cases where an ongoing deactivation occurs after termination of the induction period (e.g., LaKEMT/4). Nevertheless, they are useful for a semi-quantitative discussion of trends. The ratio of end-of-run conversions, $X_{\text{E-Bz, LaNa-zeolite}}/X_{\text{E-Bz, LaK-zeolite}}$, declines in the order Y/2 ≥ Y/3 > X/1 > EMT/4.

TABLE 2

Ethylbenzene Disproportionation on La*M* and H*M* Zeolites at 453 K

Sample designation	$X_{\text{E-Bz}}$ in the stationary state, in %	c_{OH} in the large cages, in (mmol/g)	c_{La} in the large cages, in (mmol/g)
LaNaX/1	8.5	0.90	0.45
LaKX/1	3.3	0.70	0.35
LaNaY/2	9.0	1.05	0.55
LaKY/2	2.0	0.45	0.40
LaNaY/3	10.0	1.15	0.60
LaKY/3	2.8	0.55	0.35
LaNaEMT/4	13.2	1.35	0.50
LaKEMT/4	6.9	1.00	0.40
72HNaY/2	3.8	1.25	
75HKY/2	2.8	0.57	
55HNaY/2	2.0	0.94	
54HKY/2	0.2	0.42	

Note. "$X_{\text{E-Bz}}$ in the stationary state" is the end-of-run conversion from Figs. 1 and 2, "c_{OH} in the large cages" is the concentration of bridging OH groups in the large cages (accuracy of ±10%) of the respective zeolite determined by ^{1}H MAS NMR spectroscopy after dehydration in vacuum at 523 or 673 K, and "c_{La} in the large cages" is the concentration of lanthanum cations in the large cages (accuracy of ±10%) of the as-exchanged La*M* zeolites determined by ^{139}La NMR spectroscopy.

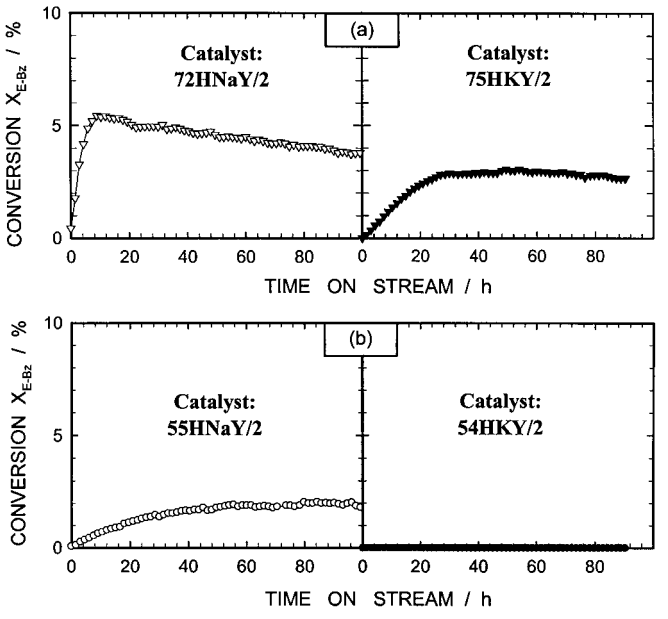

FIG. 2. Ethylbenzene disproportionation on zeolites 72HNaY/2 and 75HKY/2 (a) and on zeolites 55HNaY/2 and 54HKY/2 (b). Conversion in dependence of time on stream at a reaction temperature of 453 K.

The conversion of ethylbenzene on the two pairs of the H*M* forms of the active Y/2 zeolite in dependence of time on stream is shown in Fig. 2. In agreement with the behavior of La*M* zeolites, the HKY/2 zeolites are less active in the (quasi-)stationary state than the respective HNaY/2-zeolites. In the case of zeolites 72HNaY/2 and 75HKY/2 (Fig. 2a) differences in the duration of the induction period similar to those for La*M* zeolites were found.

Isomerization of n-Octane

LaNaY/2 and LaKY/2, i.e., the La*M* zeolite pair with the most pronounced activity differences in ethylbenzene disproportionation, were tested as catalysts in another acid-catalyzed reaction, viz. the skeletal isomerization of *n*-octane. For this reaction, the acid zeolites had to be made bifunctional, and this was done by physically admixing Pd/γ-Al_2O_3 ("mixed powder technique" (22)).

The conversions of *n*-octane achieved at 473 K are depicted in the left-hand part of Fig. 3. The same effect as in the ethylbenzene disproportionation is again observed: Pd/LaNaY/2 gives an *n*-octane conversion of approximately 3%, which declines to about 2% within 10 h on stream. No conversion at all occurs on Pd/LaKY/2. Raising the temperature to 513 K (right-hand part of Fig. 3) results in some small conversion on Pd/LaKY/2, but under these new conditions, too, Pd/LaNaY/2 is clearly more active. As expected (2), skeletal isomerization of *n*-octane to iso-octanes was the sole reaction observed under the relatively mild

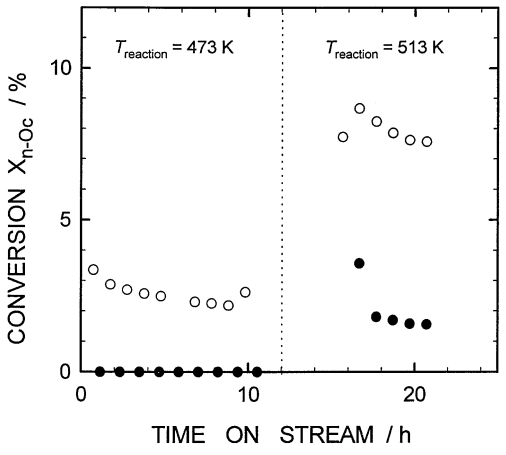

FIG. 3. Conversion of *n*-octane in hydrogen on Pd/LaNaY/2 (open circles) and Pd/LaKY/2 (full circles) at two reaction temperatures.

conditions applied; i.e., no hydrocraking took place. Similar differences in the skeletal isomerization of *n*-octane were obtained on Pd/H*M*Y/2 zeolites with sodium and potassium as alkali cation *M*. At the reaction temperature of 513 K, conversions of *n*-octane of 11.0 and 0.9% were found for zeolites Pd/72HNaY/2 and Pd/75HKY/2, respectively, and of 5.8 and 0.2% for zeolites Pd/55HNaY/2 and Pd/54HKY/2, respectively (not shown).

IR Spectroscopy

Qualitatively, the typical IR spectra of acidic faujasites and EMT zeolites were obtained. As an example, Fig. 4 shows the region of the OH stretching vibrations for zeolites LaNaX/1 and LaKX/1. The spectra were taken after dehydration at 523 K before (solid lines) and after (dashed lines) adsorption of pyridine. According to the generally accepted assignment (23, 24), the bands at approximately 3620 and 3540 cm^{-1} originate from bridging OH groups in the supercages and in the small cages, respectively, whereas the band at approximately 3570 cm^{-1} is characteristic of nonacidic $LaOH^{2+}$ or $La(OH)_2^+$ groups. In agreement with this assignment, the bands at approximately 3620 cm^{-1} disappear upon the admission of pyridine, whereas the Brønsted acid sites in the small cages are not neutralized by the bulky base pyridine. The important information in the present context comes from a comparison of the bands at approximately 3620 cm^{-1} in both spectra (solid lines): Clearly, this band is more intense in the spectrum of LaNaX/1 than in that of LaKX/1, indicating that the concentration of Brønsted acid sites in the large cages, and hence of catalytic sites accessible to the reactant hydrocarbons used in the catalytic experiments, is significantly higher in the LaNa form of zeolite X/1, even though the degree of lanthanum exchange is essentially the same for both samples (cf. Table 1).

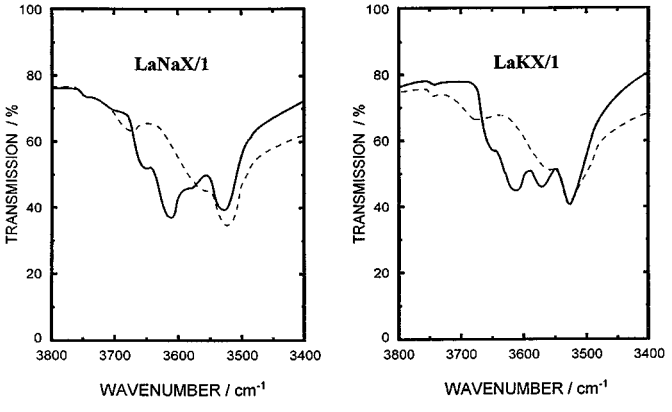

FIG. 4. Stretching vibration region of the IR spectra for zeolites LaNaX/1 and LaKX/1 after calcination at 523 K before (solid lines) and after (dashed lines) adsorption of pyridine.

^{1}H MAS NMR Spectroscopy

To collect more quantitative information on the concentrations of Brønsted acid sites in the large and small cages, ^{1}H MAS NMR spectra of the zeolites calcined at 523 K were taken. In Figs. 5a and 5b, these spectra are depicted, respectively, for the catalyst couple LaNaX/1 and LaKX/1.

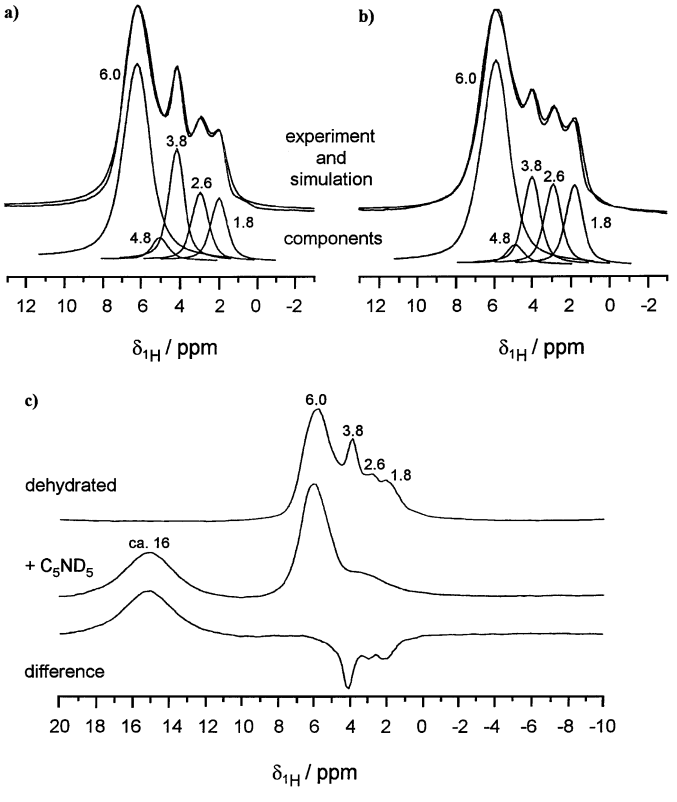

FIG. 5. ^{1}H MAS NMR spectra of dehydrated (523 K) zeolites LaNaX/1 (a) and LaKX/1 (b) and of zeolite LaNaX/1 after adsorption of perdeuterated pyridine (c), recorded at a resonance frequency of 400.13 MHz with a sample spinning rate of 10 kHz.

Also shown in this figure are the spectra after their decomposition using the BRUKER software WINFIT. Based on our earlier work (12, 25), the signals are assigned as follows: The line at 1.8 ppm originates from silanol groups, the line at 2.6 ppm from OH groups residing on extra-framework aluminum species, the lines at 3.8 and 4.8 ppm from bridging OH groups in the large and small cages, respectively, and the broad signal at 6.0 ppm from OH groups bound to lanthanum cations. The relatively large shift of this signal is not indicative of a high acid strength, but rather of hydrogen bonding to framework oxygen atoms contiguous to the lanthanum-bound OH groups (12).

Upon adsorption of perdeuteropyridine in sample LaNaX/1 (Fig. 5c, center spectrum), the signal at 3.8 ppm is no longer present, which is consistent with its assignment to Brønsted acid sites pointing into the supercages. The new signal appearing at approximately 16 ppm originates from the protonated probe molecule, and this is again in-line with the Brønsted acid nature of the accessible bridging OH groups in zeolite LaNaX/1. At the same time, these findings exclude a contribution of acidic OH groups to the signal at 6.0 ppm in the spectra of LaMX/1.

^{1}H MAS NMR investigations of weight-controlled samples carried out in the absolute intensity mode with an external intensity standard and with decomposition of the spectra as demonstrated in Figs. 5a and 5b, yielded the concentrations of accessible bridging OH groups of the La*M* zeolites, as listed in column 3 of Table 2 (accuracy of ±10%). These concentrations show the same trends as qualitatively found by IR spectroscopy (*vide supra*). In each case, the lanthanum exchange and subsequent thermal treatment led to a higher concentration of accessible Brønsted acid sites (signal at 3.8 ppm) in the LaNa form than in the respective LaK form. Figure 6 shows the ^{1}H MAS NMR spectra of zeolites H*M*Y/2 (*M*: Na, K), which are dominated by signals at 3.8 and 4.8 ppm due to bridging OH groups in the large and in the small cages, respectively. Adsorption of perdeuteropyridine indicated that only the OH groups responsible for the signal at 3.8 ppm are fully accessible for the probe molecule applied. Considering the intensity ratios of the lines at 3.8 and 4.8 ppm, again, the potassium-containing zeolites 75HKY/2 (Fig. 6b) and 54HKY/2 (Fig. 6d) show significantly weaker signals of accessible Brønsted acid sites in the large cages (signal at 3.8 ppm) than zeolites 72HNaY/2 (Fig. 6a) and 55HNaY/2 (Fig. 6c). The corresponding concentrations of bridging OH groups in the large cages are given in column 3 of Table 2. This finding indicates a general influence of the nature of the residual alkali cations on the distributions of bridging OH groups in large and small cages.

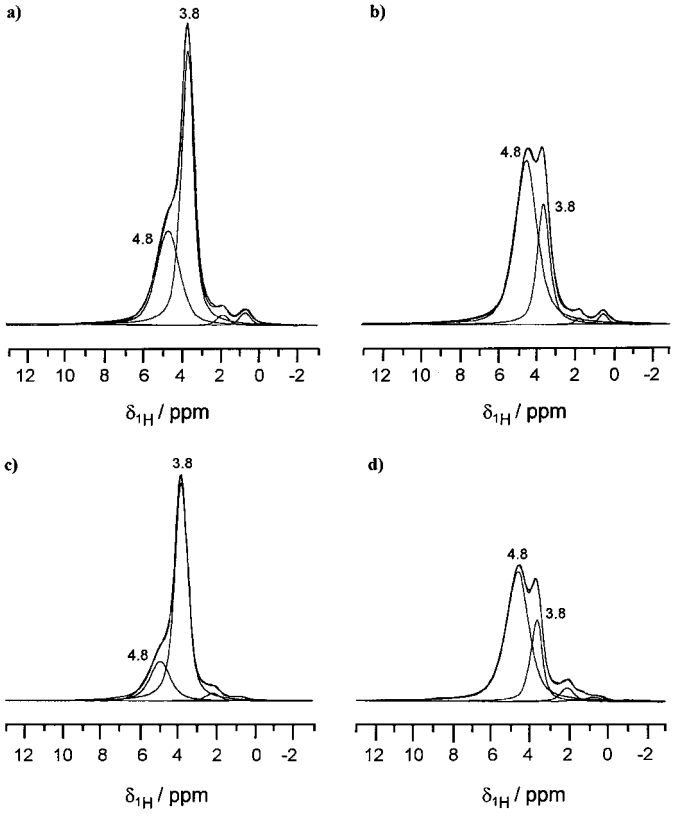

FIG. 6. ^{1}H MAS NMR spectra of dehydrated (673 K) zeolites 72HNaY/2 (a), 75HKY/2 (b), 55HNaY/2 (c), and 54HKY/2 (d), recorded at a resonance frequency of 400.13 MHz with a sample spinning rate of 10 kHz.

^{139}La NMR Spectroscopy

It has been shown previously that ^{139}La NMR spectroscopy is a useful tool for the investigation of the location and migration of lanthanum cations in zeolites (11, 26). Lanthanum nuclei with a spin of $I = 7/2$ are involved in quadrupolar interactions with electric field gradients caused by electric charges in the surrounding of the resonating nuclei. These electric field gradients are small for a symmetric charge distribution, i.e., for fully hydrated and mobile lanthanum cations in the large cavities. Conversely, they are large for a nonsymmetric charge distribution as, e.g., for lanthanum cations located close to the centers of six-membered oxygen rings, such as positions SI′ in the sodalite cages. Previous ^{139}La NMR investigations on hydrated LaNaY zeolites yielded spectra consisting of (i) a signal with a linewidth of 12 ± 2 kHz due to fully hydrated lanthanum cations in the supercages and (ii) a signal with a linewidth of 190 ± 10 kHz caused by lanthanum cations located in sodalite cages. The strong broadening of signal (ii) renders its detection difficult. On the other hand, the intensity of signal (i) could be used for a quantitative determination of the lanthanum cations in the supercages of hydrated zeolites Y (accuracy of ±10%) (11, 26, 27). In the present study, a hydrated LaNaY zeolite was used as an external intensity standard, the lanthanum cations of which were subjected to the same quadrupolar interactions as those in zeolites X/1, Y/2, Y/3, and EMT/4.

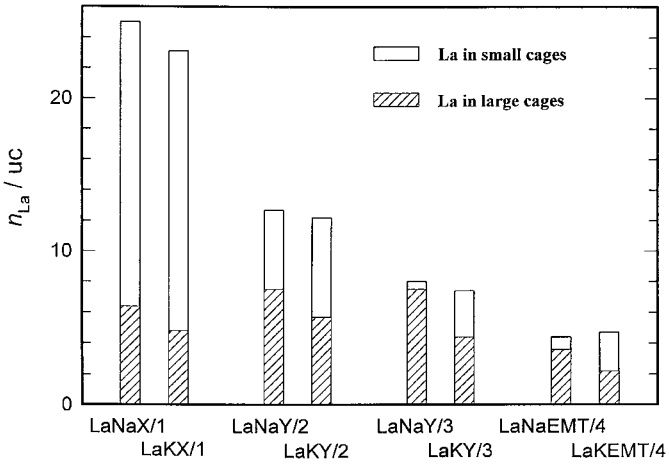

FIG. 7. Numbers of lanthanum cations per unit cell introduced into zeolites X/1, Y/2, Y/3, and EMT/4 by cation exchange in aqueous $La(NO_3)_3$ solution (full height of bars) and numbers of lanthanum cations per unit cell in the large cages (shaded portion of bars, see text) of the as-exchanged samples determined by the intensities of signal (*i*) in the ^{139}La NMR spectra. The white portions of the bars give the numbers of lanthanum cations per unit cell located in the small cages.

In Fig. 7, the total numbers of lanthanum cations in the as-exchanged La*M* zeolites as determined by ICP-AES (full height of bars) are shown. The shaded portions of the bars give the numbers of fully hydrated and mobile lanthanum cations in the large cages derived by the ^{139}La NMR intensities of signal (*i*). Consequently, the white portions of the bars correspond to the numbers of lanthanum cations in the small cages. Considering these values, the numbers of lanthanum cations in the supercages of all as-exchanged LaNa-zeolites are higher than those of the corresponding LaK zeolites. In other words, already in the as-exchanged samples, a migration of lanthanum cations to positions in the small cages takes place, and to what extent this occurs depends on the nature of the residual alkali cations.

^{29}Si MAS NMR Spectroscopy

Applying ^{29}Si MAS NMR spectroscopy, Chao and Chern (28) found that ion exchange of zeolite NaY with K, Ca, Sr, Ba, La, and Ce cations and subsequent dehydration brings about a high-field shift of the Si(*n*Al) signals, where *n* is the number of aluminum atoms in the second coordination sphere of the resonating silicon atoms. This high-field shift was explained by a local strain of framework SiO_4 tetrahedra in the neighborhood of extra-framework positions occupied by large cations.

Figure 8 shows ^{29}Si MAS NMR spectra of zeolite X/1 in the pure Na (a) and K forms (b) and in the as-exchanged LaNa (c) and LaK forms (d). The spectrum of zeolite NaX/1 (Fig. 8a) consists of lines at chemical shifts of −84.0, −88.5, −93.5, and −98.0 ppm (accuracy of ±0.5 ppm) originating from Si(*n*Al) atoms with $n = 4$, 3, 2, and 1, respectively (17). Replacing the sodium cations (diameter: 0.204 nm (29)) by the larger potassium cations (diameter: 0.302 nm (29)) results in a high-field shift of the Si(*n*Al) signals by at least 2 ppm (cf. Figs. 8a and 8b), indicating a change in the local geometry of the SiO_4 tetrahedra. This effect is even more pronounced after the exchange with lanthanum cations (diameter: 0.232 nm (29)). In the spectra of the as-exchanged zeolites LaNaX/1 (Fig. 8c) and LaKX/1 (Fig. 8d), the Si(*n*Al) signals are high-field shifted by approximately 5 ppm. It is interesting to note that the high-field shifts can already be observed in the as-exchanged samples, i.e., prior to the first thermal treatment. The exchange-induced high-field shifts observed in the ^{29}Si MAS NMR spectra of zeolites Y/2, Y/3, and EMT/4 (not shown) are significantly smaller (approximately 1 ppm) than those shown in Fig. 8 for zeolite X/1. Gaare and Akporiaye (30) observed a selective exchange of cations close to the Si(4Al) sites in zeolite X that may cause the difference in the exchange-induced high-field shifts of the ^{29}Si MAS NMR signals of zeolites studied in the present work. In addition, the absolute numbers of lanthanum atoms exchanged into zeolite X/1 is by a factor of 2 to 5 larger than in all other zeolites (see Table 1).

^{27}Al MAS NMR and DOR NMR Spectroscopy

Previous studies have demonstrated that ^{27}Al MAS NMR spectroscopy of zeolites is sensitive to the oxygen

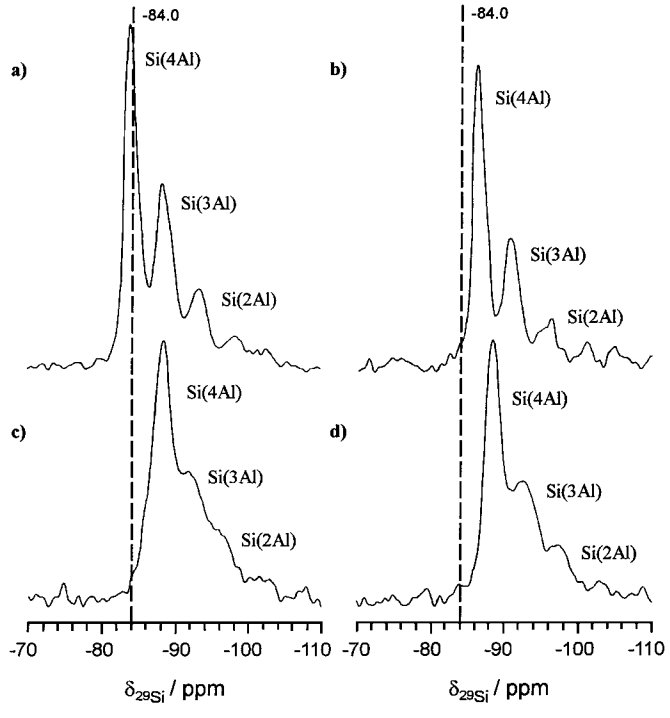

FIG. 8. ^{29}Si MAS NMR spectra of zeolites NaX/1 (a) and KX/1 (b) and of the as-exchanged zeolites LaNaX/1 (c) and LaKX/1 (d), recorded at a resonance frequency of 79.5 MHz with a sample spinning rate of 3.5 kHz.

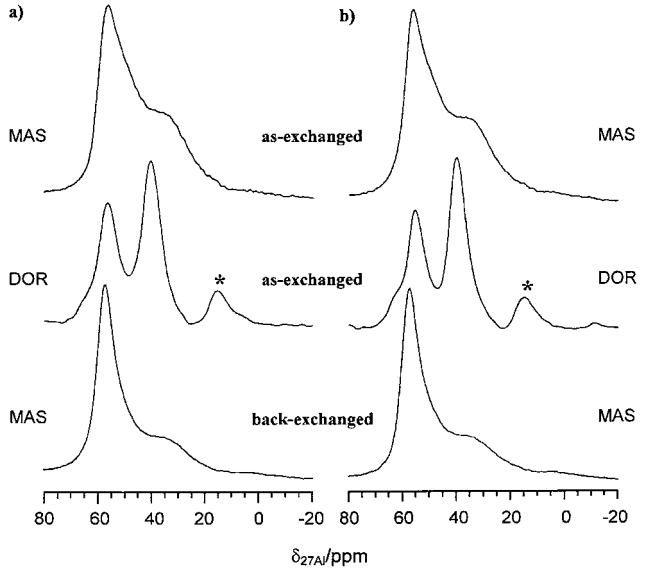

FIG. 9. ^{27}Al MAS and DOR NMR spectra of zeolites LaNaX/1 (a) and LaKX/1 (b) in the as-exchanged state (top and center) and after back-exchange of the lanthanum cations with sodium in an aqueous $NaNO_3$ solution (bottom). The asterisks designate spinning sidebands in the DOR spectra.

coordination of aluminum atoms as well as to the strain of the framework AlO_4 tetrahedra (11, 27). Shown in Fig. 9 (top and center) are the spectra of the as-exchanged zeolites LaNaX/1 and LaKX/1. The MAS NMR (top) spectra of the as-exchanged samples are dominated by signals of tetrahedrally coordinated framework aluminum at 58 ppm and a broad signal at approximately 40 ppm with a linewidth of approximately 25 ppm. Since no signal was found at 0 ppm, the presence of extra-framework aluminum can be excluded. From investigations on homologous series of lanthanum-exchanged zeolites Y it is known that the broad signal at approximately 40 ppm is characteristic of AlO_4 tetrahedra strained by lanthanum cations located in the sodalite cages (11). Application of the DOR technique (Fig. 9, center) narrows the broad signal down to a linewidth of approximately 15 ppm, which reveals that the dominating line-broadening mechanism is second-order quadrupole interaction rather than a distribution of the chemical shift. Hence, the broad signal at 40 ppm provides independent evidence for a local strain of framework tetrahedra (AlO_4) induced by the migration of lanthanum cations to positions in the sodalite cages of the as-exchanged samples. It is noteworthy that the back-exchange of as-exchanged zeolite LaKX/1 with an aqueous $NaNO_3$ solution decreases the intensity of the broad signal by a factor of less than 2 (Fig. 9, bottom). This indicates that the migration of lanthanum cations from positions in the large cages to positions in the sodalite cages upon ion exchange in aqueous solution is a partially irreversible process.

DISCUSSION

All LaNa and HNa zeolites employed in this study were found to be catalytically more active than their respective LaK and HK counterparts, and this holds for both acid-catalyzed reactions (cf. Figs. 1 to 3). IR and ^{1}H MAS NMR spectroscopy on the dehydrated zeolites revealed that the concentration of bridging OH groups in the large cages, i.e., of Brønsted acid sites accessible to the hydrocarbons, was at least 20% lower in the LaK forms than in the respective LaNa forms (cf. Table 2, column 3). ^{139}La NMR spectroscopy of the hydrated zeolites indicated that already in the as-exchanged zeolites, the concentrations of La^{3+} ions in the large cages are clearly lower for the LaK forms than for the corresponding LaNa forms (cf. Table 2, column 4).

In Fig. 10, the concentrations of bridging OH groups in the large cages of zeolites X/1, Y/2, Y/3, and EMT/4 (from Table 2, column 3) are plotted versus the concentrations of lanthanum cations in the large cages of the as-exchanged zeolites in their LaNa and LaK forms (from Table 2, column 4). Despite some scattering, a correlation appears to exist. Roughly, about two bridging OH groups were formed according to the Hirschler/Plank mechanism per lanthanum cation remaining in the large cages of the as-exchanged samples. Hence, lanthanum species like $La(OH)_2(H_2O)_n^+$ should be formed, causing the ^{1}H MAS NMR signal at 6 ppm. The measured concentrations of accessible bridging OH groups can as well be correlated with the experimentally observed conversions of ethylbenzene in the (quasi-)stationary stage of the reaction (see Fig. 11). This latter result is in principle agreement with earlier data reported by Karge *et al.* for systematically varied mordenites (31) and faujasites (1) containing different alkaline earth cations.

More information concerning the reasons for the different concentrations of lanthanum cations in seemingly

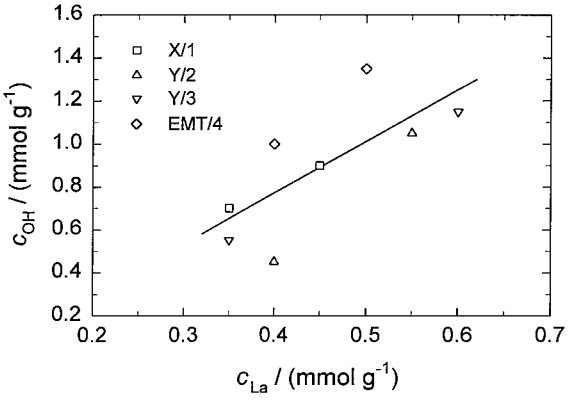

FIG. 10. Concentration of bridging OH groups in the large cages of zeolites La*M*X/1, La*M*Y/2, La*M*Y/3, and La*M*EMT/4 (*M* stands for Na or K) determined by ^{1}H MAS NMR spectroscopy versus the concentration of lanthanum cations in the large cages of the as-exchanged LaNa and LaK zeolites.

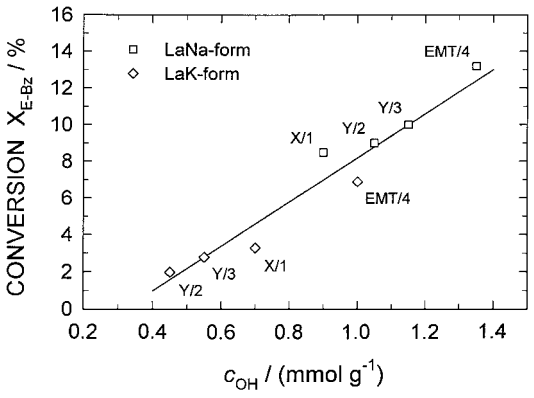

FIG. 11. Conversion of ethylbenzene in the stationary state (Table 2, column 2) versus the concentration of accessible bridging OH groups in the large cages of the dehydrated LaNa and LaK zeolites X/1, Y/2, Y/3, and EMT/4 determined by ^{1}H MAS NMR spectroscopy (Table 2, column 3).

analogous LaNa and LaK zeolites came from ^{29}Si and ^{27}Al NMR spectroscopy: High-field shifts of the signals due to SiO_4 and AlO_4 tetrahedra indicated local framework strains. As shown in previous studies, such strains may be induced by the migration of lanthanum cations from positions in the large cages into the small cages (11). According to Shy *et al.* (32), a migration of lanthanum cations to positions SI in the hexagonal prisms can be excluded. In addition, no systematic variation of the unit cell constant with increasing lanthanum content was found by these authors. Since in the present study, the high-field shifts of the ^{29}Si MAS NMR signals were already observed for the as-exchanged samples, the corresponding cation migration influences the numbers of multivalent cations that are available for the formation of accessible Brønsted acid sites according to the Hirschler/Plank mechanism during the first thermal treatment. Lanthanum migration into the small cages is induced by the presence of potassium cations. The diameter of potassium cations (0.302 nm) is large in comparison with that of lanthanum (0.232 nm) and sodium (0.204 nm) cations (29). In the as-exchanged LaK zeolites X/1, Y/2, Y/3, and EMT/4, the repulsive interactions of the large potassium cations enhance the migration of lanthanum cations into the small cages. The importance of the repulsive interactions for the cation distribution in the small cages of zeolite Y was discussed earlier by van Dun and Mortier (33).

On the basis of the experimental results obtained in the present study, we are led to interpret the activity differences between the LaNa and the LaK forms of the zeolite catalysts primarily in terms of different concentrations of *accessible* Brønsted acid sites, i.e., bridging OH groups in the large cages of faujasite and zeolite EMT. This explanation is strongly supported by our investigations of the HNaY/2 and HKY/2 zeolites, which show similar differences in the catalytic behavior and *concentrations of bridging OH groups in the large cages*. In both cases, the presence of the large potassium cations hinders the formation of accessible Brønsted acid sites in the large cages, i.e., bridging OH groups are preferentially formed in the small cages where they are not accessible for the hydrocarbons used as reactants in this study.

There is, of course, at least one alternative factor that might influence the catalytic activity of La*M* and H*M* zeolites, viz. a *lower strength* of the Brønsted acid sites in the potassium-containing zeolites than in their sodium-containing counterparts, as invoked by O'Donoghue and Barthomeuf (7) and Chen *et al.* (8). According to Sanderson's principle of electronegativity equalization, decreasing partial charges residing at the hydrogen should cause a *lower strength* of bridging OH groups in LaK and HK zeolites than in LaNa and HNa zeolites. The experimental findings of O'Donoghue and Barthomeuf (7) and Chen *et al.* (8), however, which were related to Sanderson's principle of electronegativity equalization, can also be rationalized in terms of differences in the distribution of accessible Brønsted acid sites. In both papers, equal numbers of accessible bridging OH groups in the large cages of zeolites Y exchanged with various alkali cations were tacitly assumed. However, in the light of our results with the HNaY/2 and HKY/2 zeolites, this assumption is by no means justified. We would rather prefer to interpret, in the first place, the different catalytic activities found in Ref. (7) for HNaY and HKY zeolites in the dehydration of 2-propanol and the different amounts of strongly adsorbed pyridine found in Ref. (8) after desorption at elevated temperatures in terms of different distributions of the bridging OH groups over the small and large cages. Of course, this is not meant to claim that differences in the acid strength do not exist at all or do not influence the catalytic and adsorptive behavior at all. Unfortunately, the data presented in the present paper do not make it possible to sort out, in a quantitative manner, the contribution of the strength of the Brønsted acid sites and their concentration in the large cages. By the combined application of IR- and multinuclear NMR-spectroscopic techniques we did, nevertheless, demonstrate unambiguously that in La*M* and H*M* zeolites with large and small cages, such as FAU and EMT, the location of the Brønsted acid sites and, hence, their accessibility for typical hydrocarbon reactants depend to a significant extent on the nature of the residual alkali cation *M*.

CONCLUSIONS

As shown in this study, the nature of the residual alkali cations in lanthanum-exchanged zeolites and in H zeolites can exert a pronounced influence on the activity of these materials in typical acid-catalyzed reactions. IR spectroscopy in the OH stretching region and ^{1}H MAS NMR spectroscopy on the dehydrated materials strongly suggest that the lower activity of the LaK and HK zeolites used in this investigation as compared to that of their

LaNa and HK counterparts is due to a lower concentration of Brønsted acid sites in the large cages. ^{139}La NMR spectroscopy of the as-exchanged materials indicated that, already before any thermal treatment, the presence of potassium ions induces some migration of lanthanum cations into the small cages, and this was corroborated by framework strain found in the same zeolites by ^{27}Al and ^{29}Si MAS NMR spectroscopy.

ACKNOWLEDGMENTS

Financial support by Deutsche Forschungsgemeinschaft, Fonds der Chemischen Industrie and Max-Buchner-Forschungsstiftung is gratefully acknowledged.

REFERENCES

1. Karge, H. G., Hatada, K., Zhang, Y., and Fiederow, R., *Zeolites* **3**, 13 (1983).
2. Weitkamp, J., *Ind. Eng. Chem. Prod. Res. Dev.* **21**, 550 (1982).
3. Weitkamp, J., and Ernst, S., *in* "Catalysis by Acids and Bases" (B. Imelik, C. Naccache, G. Coudurier, Y. Ben Taarit, and J. C. Vedrine, Eds.), Studies in Surface Science and Catalysis, Vol. 20, p. 419, Elsevier, Amsterdam, 1985.
4. von Ballmoos, R., Harris, D. H., and Magee, J. S., *in* "Handbook of Heterogeneous Catalysis" (G. Ertl, H. Knözinger, and J. Weitkamp, Eds.), Vol. 4, p. 1955, Wiley-VCH Weinheim, 1997.
5. Blauwhoff, P. M. M., Gosselink, J. W., Kieffer, E. P., Sie, S. T., and Stork, W. H. J., *in* "Catalysis and Zeolites" (J. Weitkamp and L. Puppe, Eds.), p. 437, Springer-Verlag, Berlin, 1999.
6. Hirschler, A. E., *J. Catal.* **2**, 428 (1963).
7. O'Donoghue, E., and Barthomeuf, D., *Zeolites* **6**, 267 (1986).
8. Chen, Y. S., Guisnet, M., Kern, M., and Lemberton, J. LK., *New J. Chem.* **11**, 623 (1987).
9. Karge, H., *Z. Phys. Chem. (Neue Folge)* **76**, 133 (1971).
10. Hunger, M., Engelhardt, G., and Weitkamp, J., *in* "Zeolites and Related Microporous Materials: State of the Art 1994" (J. Weitkamp, H. G. Karge, H. Pfeifer, and W. Hölderich, Eds.), Studies in Surface Science and Catalysis, Vol. 84, Part A, p. 725, Elsevier, Amsterdam, 1994.
11. Hunger, M., Engelhardt, G., and Weitkamp, J., *Micropor. Mater.* **3**, 497 (1995).
12. Hunger, M., *Catal. Rev.-Sci. Eng.* **39**, 345 (1997).
13. Guth, J.-L., and Kessler, H., *in* "Catalysis and Zeolites" (J. Weitkamp and L. Puppe, Eds.), p. 1, Springer-Verlag, Berlin, 1999.
14. Delprato, F., Delmotte, L., Guth, J.-L., and Huve, L., *Zeolites* **10**, 546 (1990).
15. Baerlocher, Ch., McCusker, L. B., and Chiappetta, R., *Micropor. Mater.* **2**, 269 (1994).
16. Weitkamp, J., and Schumacher, R., *in* "Proceedings from the Ninth International Zeolite Conference" (R. von Ballmoos, J. B. Higgins, and M. M. J. Treacy, Eds.), Vol. 1, p. 353, Butterworth-Heinemann, Stoneham, MA, 1993.
17. Engelhardt, G., and Michel, D., "High Resolution Solid-State NMR of Silicates and Zeolites," p. 212, Wiley, Chichester, 1987.
18. Kunwar, A. C., Turner, G. L., and Oldfield, E., *J. Magn. Reson.* **69**, 124 (1986).
19. Karge, H. G., Ernst, S., Weihe, M., Weiss, U., and Weitkamp, J., *in* "Zeolites and Related Microporous Materials: State of the Art 1994" (J. Weitkamp, H. G. Karge, H. Pfeifer, and W. Hölderich, Eds.), Studies in Surface Science and Catalysis, Vol. 84, Part C, p. 1805, Elsevier, Amsterdam, 1994.
20. Weihe, M., Ph.D. Thesis, University of Stuttgart (1997).
21. Arsenova-Härtel, N., Haag, W. O., and Karge, H. G., *in* "Porous Materials in Environmentally Friendly Processes" (I. Kiricsi, G. Pál-Borbély, J. B. Nagy, and H. G. Karge, Eds.), Studies in Surface Science and Catalysis, Vol. 125, p. 341, Elsevier, Amsterdam, 1999.
22. Weisz, P. B., and Swegler, E. W., *Science* **126**, 31 (1957).
23. Karge, H. G., Hunger, M., and Beyer, H., *in* "Catalysis and Zeolites" (J. Weitkamp and L. Puppe, Eds.), p. 198, Springer-Verlag, Berlin, 1999.
24. Ward, J. W., *in* "Zeolite Chemistry and Catalysis" (J. A. Rabo, Ed.), ACS Monograph 171, p. 124, American Chemical Society, Washington, DC, 1976.
25. Hunger, M., Horvath, T., and Weitkamp, J., *in* "Progress in Zeolite and Microporous Materials" (H. Chon, S.-K. Ihm, and Y. S. Uh, Eds.), Studies in Surface Science and Catalysis, Vol. 105, Part B, p. 853, Elsevier, Amsterdam, 1996.
26. Herreros, B., Man, P. P., Manoli, J.-M., and Fraissard, J., *J. Chem. Soc. Chem. Commun.* 464 (1992).
27. Klein, H., Fuess, H., and Hunger, M., *J. Chem. Soc. Faraday Trans.* **91**, 1813 (1995).
28. Chao, K.-J., and Chern, J. Y., *J. Phys. Chem.* **93**, 1401 (1989).
29. Weast, R. C., "CRC Handbook of Chemistry and Physics," 74rd ed., p. 12, CRC Press, Boca Raton, FL, 1993–1994.
30. Gaare, K., and Akporiaye, D., *J. Phys. Chem. B* **101**, 48 (1997).
31. Karge, H. G., Ladebeck, J., Sarbak, Z., and Hatada, K., *Zeolites* **2**, 94 (1982).
32. Shy, D.-S., Chen, S.-H., Lievens, J., Liu, S.-B., and Chao, K.-J., *J. Chem. Soc. Faraday Trans.* **87**(17), 2855 (1991).
33. van Dun, J. J., and Mortier, W. J., *J. Phys. Chem.* **92**, 6740 (1988).